DIS3 depletion in multiple myeloma causes extensive perturbation in cell cycle progression and centrosome amplification

Vanessa K. Favasuli,[1,2*] Domenica Ronchetti,[1*] Ilaria Silvestris,[1] Noemi Puccio,[3,4] Giuseppina Fabbiano,[5] Valentina Traini,[5] Katia Todoerti,[6] Silvia Erratico,[7,8] Alessia Ciarrocchi,[3] Valentina Fragliasso,[3] Domenica Giannandrea,[9] Francesca Tumiatti,[10] Raffaella Chiaramonte,[9] Yvan Torrente,[7] Palma Finelli,[10,11] Eugenio Morelli,[2] Nikhil C. Munshi,[2] Niccolò Bolli,[1,5] Antonino Neri[12] and Elisa Taiana[5]

[1]Department of Oncology and Hemato-Oncology, University of Milan, Milan, Italy; [2]Department of Medical Oncology, Jerome Lipper Multiple Myeloma Center, Dana-Farber Cancer Institute, Boston, MA, USA; [3]Laboratory of Translational Research, Azienda USL-IRCCS di Reggio Emilia, Reggio Emilia, Italy; [4]Clinical and Experimental Medicine PhD Program, University of Modena and Reggio Emilia, Modena, Italy; [5]Hematology, Fondazione IRCCS Ca' Granda Ospedale Maggiore Policlinico, Milan, Italy; [6]Department of Pathology and Laboratory Medicine, Fondazione IRCCS Istituto Nazionale dei Tumori, Milan, Italy; [7]Stem Cell Laboratory, Department of Pathophysiology and Transplantation, University of Milan, Centro Dino Ferrari, Unit of Neurology, Fondazione IRCCS Cà Granda Ospedale Maggiore Policlinico, Milan, Italy; [8]Novystem Spa, Milan, Italy; [9]Department of Health Sciences, University of Milan, Milan, Italy; [10]Medical Genetics Laboratory, Fondazione IRCCS Ca' Granda Ospedale Maggiore Policlinico, Milan, Italy; [11]Department of Medical Biotechnology and Translational Medicine, University of Milan, Segrate, Italy and [12]Scientific Directorate, Azienda USL-IRCCS di Reggio Emilia, Reggio Emilia, Italy

VKF and DR contributed equally as first authors.

Correspondence: A Neri
antonino.neri@ausl.re.it

Received: April 4, 2023.
Accepted: July 5, 2023.
Early view: July 13, 2023.

https://doi.org/10.3324/haematol.2023.283274

Abstract

DIS3 gene mutations occur in approximately 10% of patients with multiple myeloma (MM); furthermore, *DIS3* expression can be affected by monosomy 13 and del(13q), found in roughly 40% of MM cases. Despite the high incidence of *DIS3* mutations and deletions, the biological significance of *DIS3* and its contribution to MM pathogenesis remain poorly understood. In this study we investigated the functional role of *DIS3* in MM, by exploiting a loss-of-function approach in human MM cell lines. We found that *DIS3* knockdown inhibits proliferation in MM cell lines and largely affects cell cycle progression of MM plasma cells, ultimately inducing a significant increase in the percentage of cells in the G0/G1 phase and a decrease in the S and G2/M phases. *DIS3* plays an important role not only in the control of the MM plasma cell cycle, but also in the centrosome duplication cycle, which are strictly co-regulated in physiological conditions in the G1 phase. Indeed, *DIS3* silencing leads to the formation of supernumerary centrosomes accompanied by the assembly of multipolar spindles during mitosis. In MM, centrosome amplification is present in about a third of patients and may represent a mechanism leading to genomic instability. These findings strongly prompt further studies investigating the relevance of *DIS3* in the centrosome duplication process. Indeed, a combination of *DIS3* defects and deficient spindle-assembly checkpoint can allow cells to progress through the cell cycle without proper chromosome segregation, generating aneuploid cells which ultimately lead to the development of MM.

Introduction

Multiple myeloma (MM) is a hematologic malignancy that is still incurable despite the recent introduction of a large array of innovative therapies.[1] MM is characterized by the abnormal proliferation of plasma cells (PC) in the bone marrow and has different clinical courses and a highly heterogeneous genetic background with both structural chromosomal alterations and specific gene mutations affecting the expression and the activity of both putative oncogenes and tumor suppressor genes.[2]

Among the frequently mutated genes in MM, *DIS3* has been reported to be mutated in roughly 10% of patients and to have a significant impact on clinical outcome.[3-6] Despite the

detailed overview of *DIS3* mutations, their functional consequences on the pathogenesis of MM remain largely unknown, to the point that it is still unclear whether *DIS3* behaves as an oncogene or a tumor suppressor gene.[7,8] Aberrant expression of *DIS3* has been reported in different tumor types.[7,9,10] Notably, monosomy 13 and del(13q), which occur in approximately 40% of MM cases, could affect *DIS3* expression.[11,12] *DIS3* encodes for a highly conserved ribonuclease[13-15] that endows the catalytic activity to the exosome, a multi-subunit complex that processes and degrades RNA for gene expression regulation, mRNA quality control, and small RNA processing.[16,17] Moreover, studies in *Schizosaccharomyces pombe* have revealed functions of *DIS3* in chromosome segregation,[18,19] cell cycle progression,[20,21] and spindle assembly.[22] The involvement of *DIS3* in cell cycle regulation has also been demonstrated in *Drosophila melanogaster*. In addition, *DIS3* is required for the development of a multicellular organism participating in cell type-specific RNA turnover.[23] In humans, *DIS3* has been described to shape the RNA polymerase II transcriptome by degrading a variety of unwanted transcripts.[24] Data concerning the functional role of *DIS3* in myeloma are limited to a recent study showing that *DIS3* depletion in different cell types, including malignant PC, causes a pervasive accumulation of DNA:RNA hybrids that induce genomic DNA double-strand breaks, eventually leading to genomic instability by increasing mutational load.[25]

In this study, we aimed to expand our knowledge on the biological role of *DIS3* in MM by investigating the functional consequences of its depletion in myeloma cells. Our data indicate that *DIS3* silencing causes marked perturbations in cell cycle progression and the process of mitosis.

Methods

Full details of quantitative real-time polymerase chain reactions, cell cycle analysis and apoptosis, immunofluorescence, gapmeR design and gymnotic delivery, proteomic assays, and gene expression analysis are provided in the *Online Supplementary Methods*.

Multi-omics data from the CoMMpass study

Multi-omics data about bone marrow MM samples at baseline (BM_1) were freely accessible from the Multiple Myeloma Research Foundation (MMRF) CoMMpass study (*https://research.themmrf.org/*) including more than 1,000 MM patients from several worldwide sites and retrieved from the Interim Analysis 15a (MMRF_CoMMpass_IA15a, accessed on 16 October 2020). Details about the molecular and clinical data of the CoMMpass cohort selected for the present study are provided in the *Online Supplementary Methods.*

Statistical and survival analyses

Wilcoxon rank-sum and Kruskal-Wallis tests were applied to assess patterns of differential expression between two or multiple molecular groups. The Dunn test was used for pairwise comparisons. *P* values were corrected using the Benjamini-Hochberg method, and adjusted *P* values <0.05 were considered statistically significant. Survival analyses were performed as described in the *Online Supplementary Methods*.

Multiple myeloma cell lines and drugs

The AMO-1 cell line was kindly provided by Dr. C. Driessen (University of Tubingen, Germany). NCI-H929 and U266 cell lines were purchased from DSMZ, which certified authentication performed by short tandem repeat DNA typing. All human MM cell lines (HMCL) were immediately frozen and used from the original stock within 6 months. HMCL were cultured in RPMI-1640 medium (Gibco®, Life Technologies, Carlsbad, CA, USA) supplemented with 10% fetal bovine serum, 50 U/mL penicillin, and 50 μg/mL streptomycin (Gibco®), at 37°C in 5% CO_2 atmosphere, and routinely tested to rule out mycoplasma contamination.

For cell cycle analyses, cells were synchronized with Synchroset kit (EuroClone, Milan, Italy). For mitotic analyses, cells were synchronized with RO-3306 and MG-132 (Selleckchem, Aurogene, Rome, Italy).

Primary patients' cells

$CD138^+$ cells were isolated from the bone marrow aspirates of MM patients by Ficoll-Hypaque (Lonza Group, Basel, Switzerland) density gradient sedimentation, followed by antibody-mediated positive selection using anti-CD138 magnetic activated cell separation microbeads (Miltenyi Biotech, Gladbach, Germany). The purity of immunoselected cells was assessed by flow-cytometry analysis using a phycoerythrin-conjugated CD138 monoclonal antibody and standard procedures. $CD138^+$ cells from MM patients were seeded and cultured in RPMI-1640 medium (Gibco®, Life Technologies) supplemented with 20% fetal bovine serum (Lonza Group Ltd) and 1% penicillin/streptomycin (Gibco®, Life Technologies).

Ethics approval and consent to participate

Written informed consent to participation in the study was obtained from all patients in accordance with the Declaration of Helsinki. The study was approved by the Ethical Committee of the Fondazione IRCCS Ca' Granda Ospedale Maggiore Policlinico (N. 575, 03/29/2018).

Results

DIS3 expression in multiple myeloma correlates with molecular subtypes

To gain insight into the role of *DIS3* in MM, we started by exploring its expression in pathological samples compared

to normal controls. In detail, we investigated *DIS3* expression levels in a proprietary, publicly available, RNA dataset profiled by microarrays that includes four healthy donors, 130 MM patients, 24 cases of primary plasma cell leukemia (PCL), and 12 cases of secondary PCL (GSE66293). Considering that *DIS3* expression levels could be affected by the presence of chromosome 13 deletion (del13), we stratified patients based on the presence of this molecular lesion. We found that patients with MM, primary PCL and secondary PCL without del13 showed significantly higher *DIS3* expression levels than normal controls; conversely, pathological samples with del13 displayed *DIS3* expression levels comparable to those of normal controls (Figure 1A).

Next, we focused on the expression pattern of *DIS3* in MM by taking advantage of a large cohort of MM patients enrolled in the MMRF CoMMpass study. To this end, we evaluated *DIS3* expression levels in PC from 774 MM patients included in the CoMMpass dataset (Figure 1B). In detail, *DIS3* expression spanned a limited range of estimated values (3.3-43.2; median: 13.16) of transcripts per million. MM patients with t(11;14) chromosomal translocation showed significantly higher *DIS3* expression levels than those of patients with other translocations (namely t(4;14), *MAF* translocations, *MYC*, double translocations) or negative for any translocations.

To assess *DIS3* expression profiles in relation to major molecular aberrations in MM, we investigated 660 MM patients of the CoMMpass cohort for whom data on expression, non-synonymous somatic mutations, and copy number alterations, collected by RNA sequencing, whole exome sequencing and next-generation sequencing-based fluorescence *in situ* hybridization, respectively, were available (*Online Supplementary Table S1*).

We observed that the presence of del13 was associated with a reduction of *DIS3* expression levels. Interestingly,

A

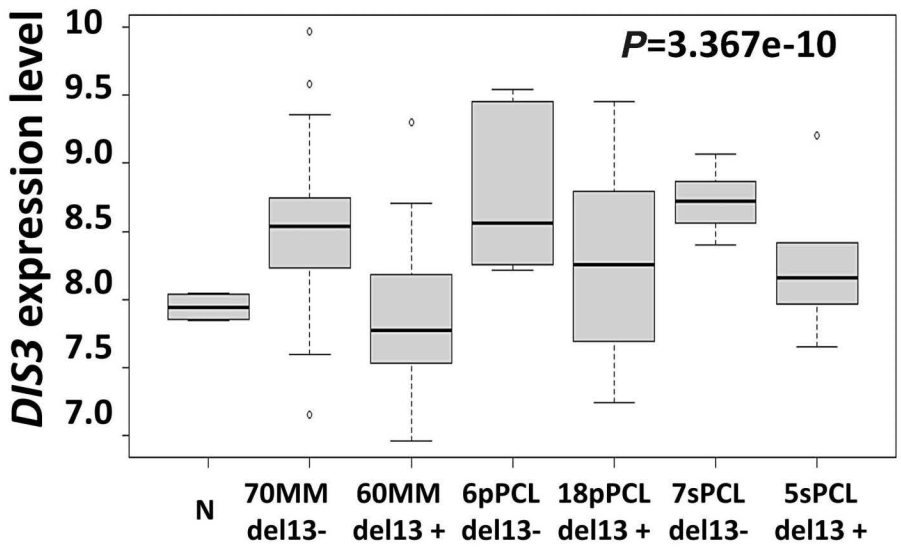

	N	MM del13-	MM del13+	pPCL del13-	pPCL del13	sPCL del13-
MM del13-	0.018					
MMdel13+	0.43	0				
pPCL del13-	0.018	0.26	0.0004			
pPCL del13+	0.13	0.037	0.0048	0.059		
sPCL del13-	0.006	0.1	0	0.34	0.015	
sPCL del13+	0.18	0.14	0.07	0.1	0.48	0.047

B

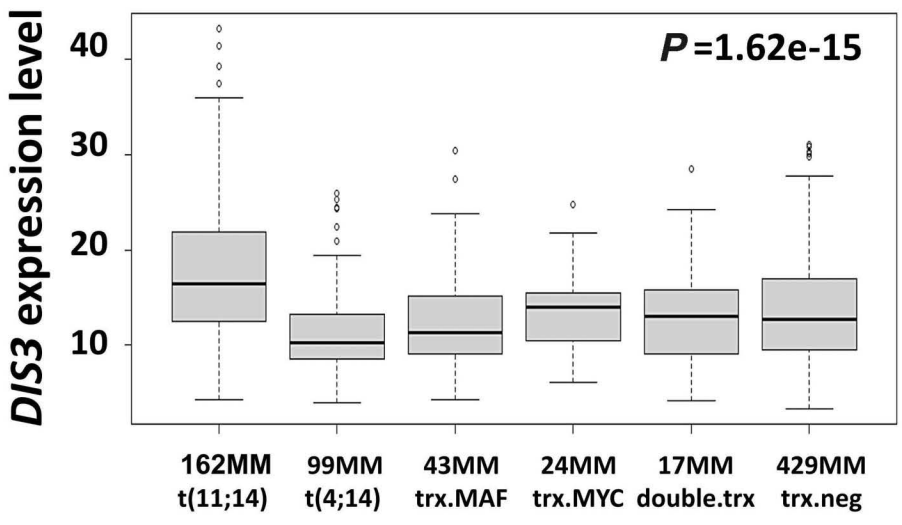

	t(11;14)	t(4;14)	Trx.MAF	Trx.MYC	Double Trx
t(4;14)	0.0000				
Trx.MAF	0.0000	0.0590			
Trx.MYC	0.0059	0.0120	0.1800		
Double Trx	0.0068	0.0500	0.3000	0.4000	
Trx NEG	0.0000	0.0000	0.1500	0.3800	0.4700

Figure 1. *DIS3* expression analysis in plasma cell dyscrasias. (A) Box plot of *DIS3* expression level in healthy donors (N) and plasma cell (PC) dyscrasias (proprietary dataset, GSE66293). The four N are RNA samples from bone marrow PC purified (>90%) from normal individuals and purchased from Voden (Medical Instruments IT). Total RNA samples from highly purified bone marrow CD138^{+} PC were profiled by Gene 1.0 ST array. (B) Box plot of *DIS3* expression level in main *IGH* translocation groups in 774 cases from the CoMMpass cohort. The Kruskal-Wallis test was applied to assess differences in expression levels between groups. The pairwise comparisons were performed by the Dunn test; statistically significant results are marked in red, bold in the tables. MM: multiple myeloma; pPCL: primary plasma cell leukemia; sPCL: secondary plasma cell leukemia; trx.MAF: *MAF* translocation, trx.MYC: *MYC* translocation, double.trx: presense of two translocations, trx.neg: absence of the considered translocations.

significantly higher *DIS3* expression levels were observed in MM patients carrying t(11;14), in particular in those without the del13 alteration (*Online Supplementary Figures S1A* and *S2A*). Significantly higher *DIS3* expression levels were also found in MM patients carrying non-synonymous somatic mutations in the *RAS/BRAF* or *FAM46C* genes, whereas lower expression levels were evidenced in samples with 1q-gain, del13, t(4;14), or a *DIS3* gene mutation (*Online Supplementary Figure S1A*). However, concerning patients with *DIS3* mutations, we observed that samples with *DIS3* hotspot mutations had higher *DIS3* expression levels than those from MM patients carryng non-hotspot *DIS3* mutations (*Online Supplementary Figure S2B*). No significant differences in *DIS3* expression levels were observed in relation to del(17p)/*TP53*, t(6;14), *MYC* or *MAF* translocations, del(1p), the occurrence of non-synonymous somatic mutations in *TRAF3* or TP53 genes, or hyperdiploid cases (*Online Supplementary Figure S1B*).

Finally, in order to investigate the relevance of *DIS3* expression levels in clinical outcome, we considered 767 MM patients from the CoMMpass dataset with available clinical data. High *versus* low expression groups were determined according to the median cutoff value for *DIS3* expression level across the entire dataset. Our data showed that *DIS3* expression levels did not affect clinical outcome in terms of either overall survival or progression-free survival (*Online Supplementary Figure S3*).

DIS3 knockdown inhibits proliferation in multiple myeloma cell lines and affects cell cycle progression and distribution

To investigate the functional role of *DIS3* in MM, we exploited a loss-of-function approach by using locked nucleic acid-gapmeR antisense oligonucleotides that trigger RNAse-H-dependent degradation of transcripts. Specifically, we designed three "in-house" sequences (g*DIS3*#2/13/15) able to recognize all three *DIS3* isoforms (*Online Supplementary Figure S4A*) and tested them in the AMO-1 HMCL by using electroporation. Among them, the g*DIS3*#13 gapmeR showed the strongest silencing efficiency (nearly 70%) after 24 h (*Online Supplementary Figure S4B*). To achieve a more pronounced and prolonged knockdown (KD) effect, we optimized its gymnotic delivery;[26] the striking downregulation of *DIS3* at both the transcriptional and protein levels obtained in different HMCL (AMO-1, NCI-H929 and U266) (Figure 2A, B), suggested that this strategy was a valuable tool for subsequent investigations.

In particular, we found that *DIS3*-KD in AMO-1, NCI-H929 and U266 cells was associated with a significant reduction of cell growth and an increase in apoptosis at 6 days after g*DIS3*#13 delivery (Figure 3A, B). Notably, HMCL showed the same phenotype at 48 h after electroporation when an RNA interference strategy was used (*Online Supplementary Figure S5*). Furthermore, *DIS3*-KD dramatically reduced (fold change 5-10) the clonogenic potential of MM cells (Figure 3C). Finally, we evaluated the biological effects of g*DIS3*#13 *ex-vivo* on primary CD138$^+$ tumor cells purified from the bone marrow of four MM patients. *DIS3*-KD led to an important alteration of cell morphology, causing cytoplasmic vacuolization, which suggests a suffering cell phenotype, and affected cell membrane integrity, converting it to one typical of apoptotic cells (Figure 3D), in agreement with the reduced viability of g*DIS3*#13-treated primary cells (*Online Supplementary Table S2*).

To inspect whether the inhibitory effects of *DIS3* silencing on proliferative potential are associated with specific changes in cell cycle progression, we analyzed AMO-1 and NCI-H929 cells silenced with g*DIS3* for 4 days. *DIS3*-KD in HMCL caused a significant increase in the number of cells in the G0/G1 phase of the cell cycle, and a decrease in the percentage of cells distributed in the S and G2/M phases, indicating G0/G1 cell cycle arrest (*Online Supplementary Figure S6*). To investigate the alterations in cell cycle progression in more detail, we synchronized HMCL using the Synchroset reagent, and followed cell cycle progression at different timepoints (*Online Supplementary Figure S7*) by collecting samples before blocking, and during and after release (*Online Supplementary Figures S8-S10*). In agreement with previous results, we found that AMO-1, NCI-H929 and U266 exhibited a modulation of the distribution of cell cycle phases after *DIS3*-KD, with a significantly increased percentage of G0/G1 phase events and a decrease of the S and G2/M phases (Figure 4A, B).

To further confirm that *DIS3*-KD results in a perturbation of cell cycle progression in HMCL, we investigated proteins that have been reported to be associated with different cell cycle checkpoints (Figure 5). In line with the cytofluorimetric analysis showing cell cycle arrest in the G0/G1 phase, *DIS3*-KD cells showed a slight increase of CCNE1 protein levels, whereas there was a decrease in the expression levels of the cyclin A protein (CCNA2), whose accumulation creates a decision window to enter the S phase and to initiate DNA replication. In agreement with a reduced G2/M phase of the cell cycle, *DIS3*-KD cells displayed reductions of both cyclin B (CCNB1) total protein and its phosphorylated fraction (pCCNB1), whose accumulation in the cyclin A/B-CDK1 complex creates a second decision window.[27,28] CCNB1 expression changes during the different phases of the cell cycle, reaching its maximum in G2/M transition. Cell entry into mitosis depends on the binding of CCNB1 to CDK1 to form the mitosis-promoting factor (MPF); CCNB1 phosphorylation promotes nuclear translocation of MPF and is important for the decisiveness and irreversibility of mitotic entry. However, MPF remains in the inactive state until phosphorylation of CDK1 (pCDK1). In our experimental condition, g*DIS3*-treated NCI-H929 and U266 cells showed a consistent reduction of the

pCDK1 fraction; pCDK1 was not affected in the g*DIS3*-*treated* AMO-1 cell line, although the total amount of CDK1 protein was reduced.

We also investigated CDC20, which is a critical checkpoint effector of mitosis and whose overexpression is associated with several types of cancer, including MM.[29,30] In our experiments, we observed an important decrease in the expression level of CDC20 protein but not of its phosphorylated fraction (pCDC20) in *DIS3*-KD cells. pCDC20 is important in the early steps of mitosis; in late anaphase and the G1 phase, CDC20 is dephosphorylated and targeted for degradation by the proteasome and is not expressed again until the S phase.

Finally, we observed a strong downmodulation of histone H3 variant CENP-A in all *DIS3*-depleted cells tested; this protein plays a fundamental role in defining centromere identity and structure and is a critical protein for the proper formation of the mitotic spindle.[31]

Transcriptional signature associated with *DIS3* silencing in the NCI-H929 cell line

In order to identify *DIS3* downstream-related pathways in MM, we investigated gene expression profiling of synchronized NCI-H929 cells after 5 days of g*DIS3*#13 gymnotic delivery. Out of 55,540 globally analyzed genes, the expression of 4,032 genes resulted significantly modulated (false discovery rate <10%) by SAM analysis. These were virtually all downregulated (3,995 genes, 99%) in *DIS3*-silenced cells and principally involved protein-coding genes (2,608 genes, 65%) and to a lesser extent long non-coding RNA (464 long non-coding RNA, 12%) (*Online Supplementary Table S3*). As expected based on previous biological results, chromosome organization, chromatin and histone modification, and cell cycle checkpoint were recognized among the top 20 most significantly enriched Gene Ontology Biological Process terms (*Online Supplementary Figure S11A*). In addition, genes involved in serine/threonine protein kinase activity, with helicase function, cata-

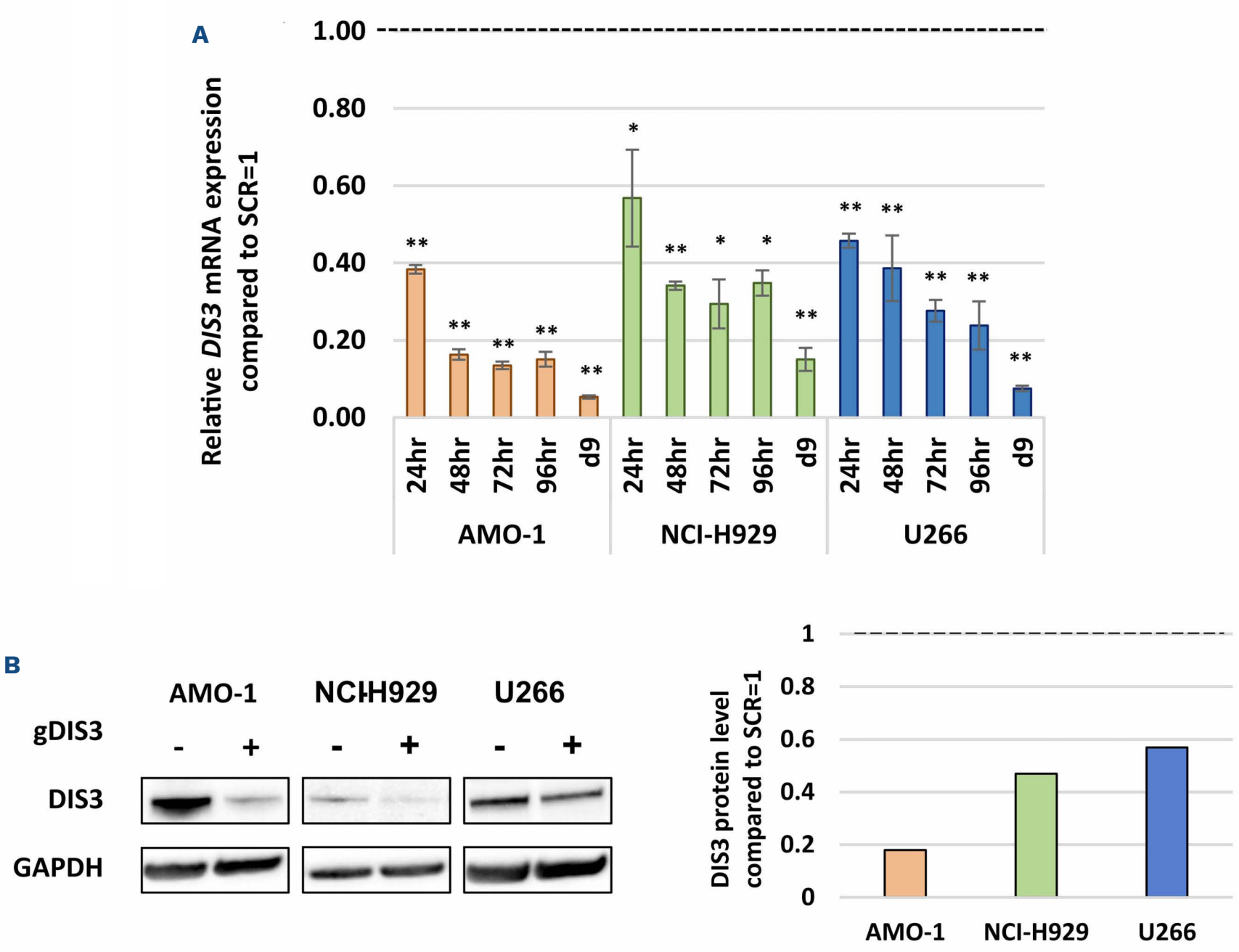

Figure 2. *DIS3* expression analysis in *DIS3*-depleted cells. (A) Quantitative real-time polymerase chain reaction analysis of *DIS3* mRNA in AMO-1, NCI-H929 and U266 cells at the indicated timepoints. *DIS3* mRNA expression is represented as $2^{-\Delta\Delta Ct}$ relative to the *GAPDH* housekeeping gene and the scrambled condition at the same timepoint used as a calibrator. **P*<0.05, ***P*<0.01, Student *t* test. (B) Western blot analyses of *DIS3*-KD in AMO-1, NCI-H929 and U266 cells. Western blot results are quantified and plotted in a histogram. SCR: scrambled condition.

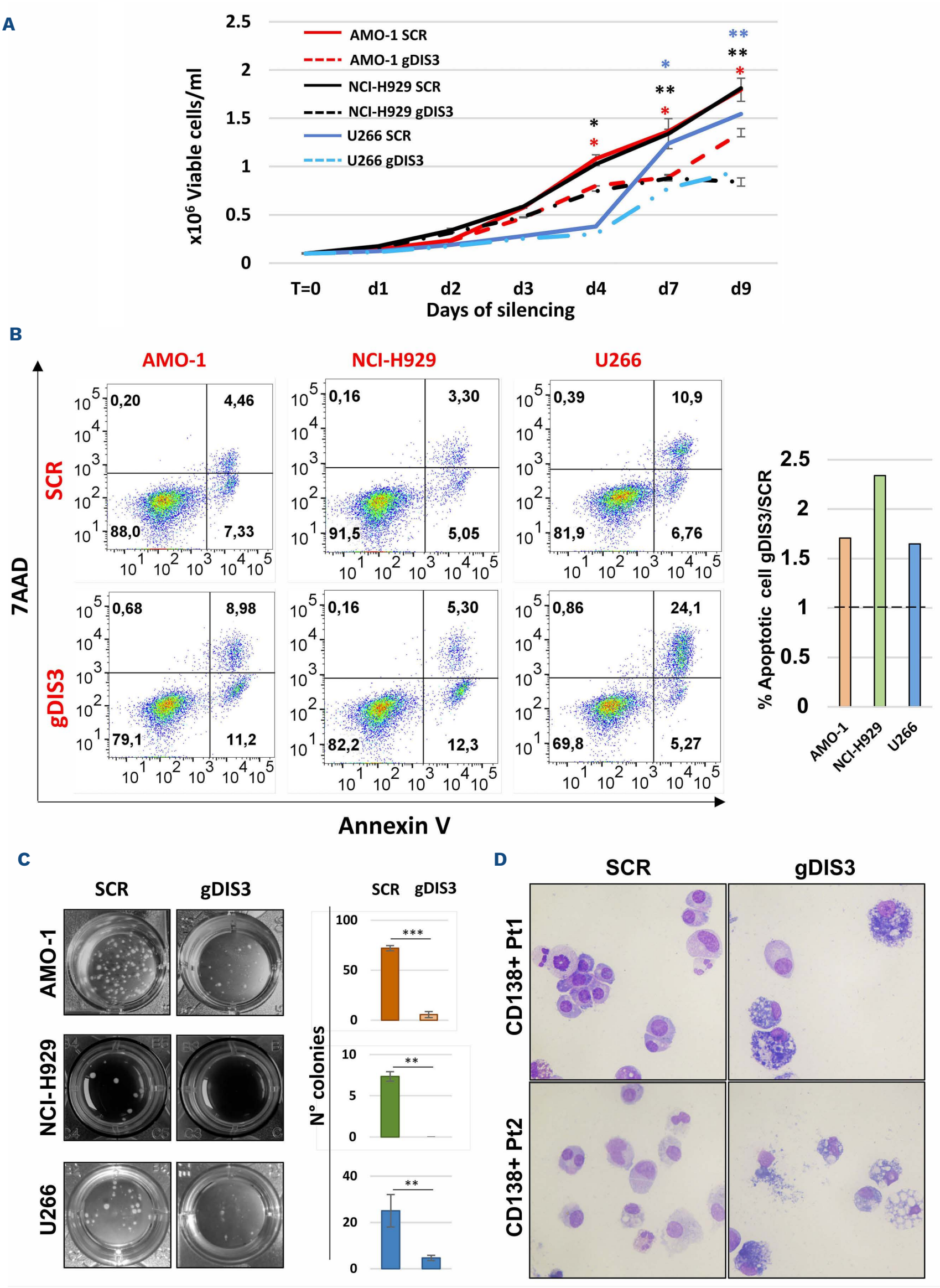

Continued on following page.

Figure 3. Functional impact of *DIS3* depletion in multiple myeloma cells. (A) Growth curves of AMO-1, NCI-H929 and U266 cells following *DIS3* silencing. (B) Flow cytometry analyses of apoptosis in AMO-1, NCI-H929 and U266 cells 6 days after treatment with g*DIS3* (5 μM). (C) Colony formation assay performed on AMO-1, NCI-H929 and U266 cells treated for 21 days with g*DIS3*; representative pictures of colonies at day 21 are also shown, ***P*<0.01, ****P*<0.001, Student *t* test. (D) Rappresentative images of May-Grünwald Giemsa staining of two CD138^{+} primary tumors treated for 6 days with g*DIS3* (50x magnification). SCR: scrambled condition; 7-AAD: 7 amino actinomycin D.

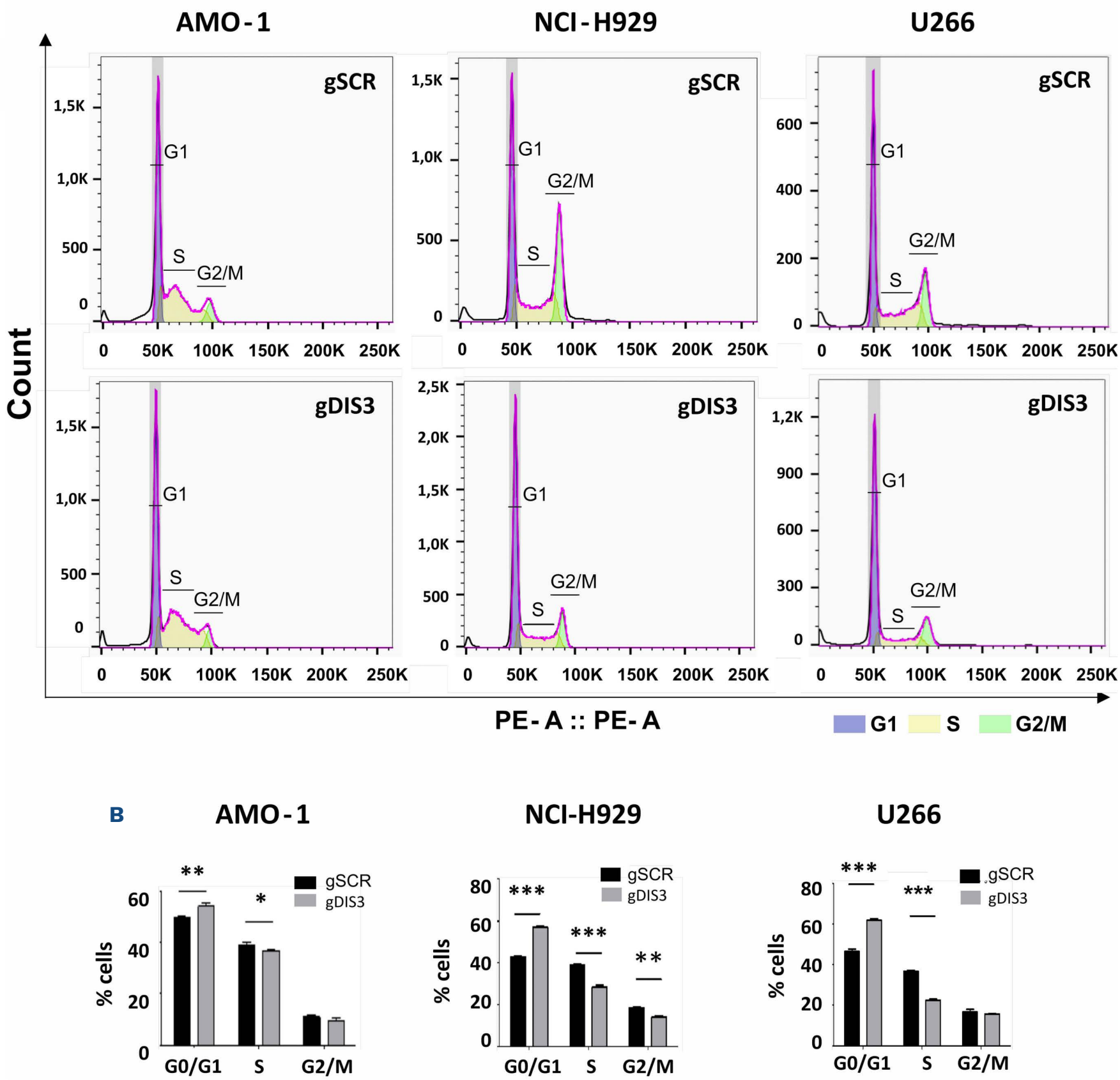

Figure 4. Cell cycle analysis in *DIS3*-depleted cells. (A) Cell cycle progression in synchronized AMO-1, NCI-H929, and U266 cells was monitored by propidium iodide staining and fluorescence activated cell sorting analysis of the DNA content of cells at 6 h after release. (B) The percentage of cell cycle distribution is represented in the histograms; the standard deviations of three replicates are reported. **P*<0.05, ***P*<0.01, ****P*<0.001, Student *t* test. SCR: scrambled condition.

lytic activity on RNA, or with tubulin binding function were evidenced in the top 20 remarkably enriched Gene Ontology Molecular Function terms under *DIS3* silencing (*Online Supplementary Figure S11B*). In particular, numerous protein-coding genes that were significantly enriched in multiple annotation categories linked to complex interactions, regarding chromosome organization and nuclear division, or molecular activities on nucleic acids and tubulin, resulted globally downregulated in *DIS3*-silenced cells (*Online Supplementary Figure S12*).

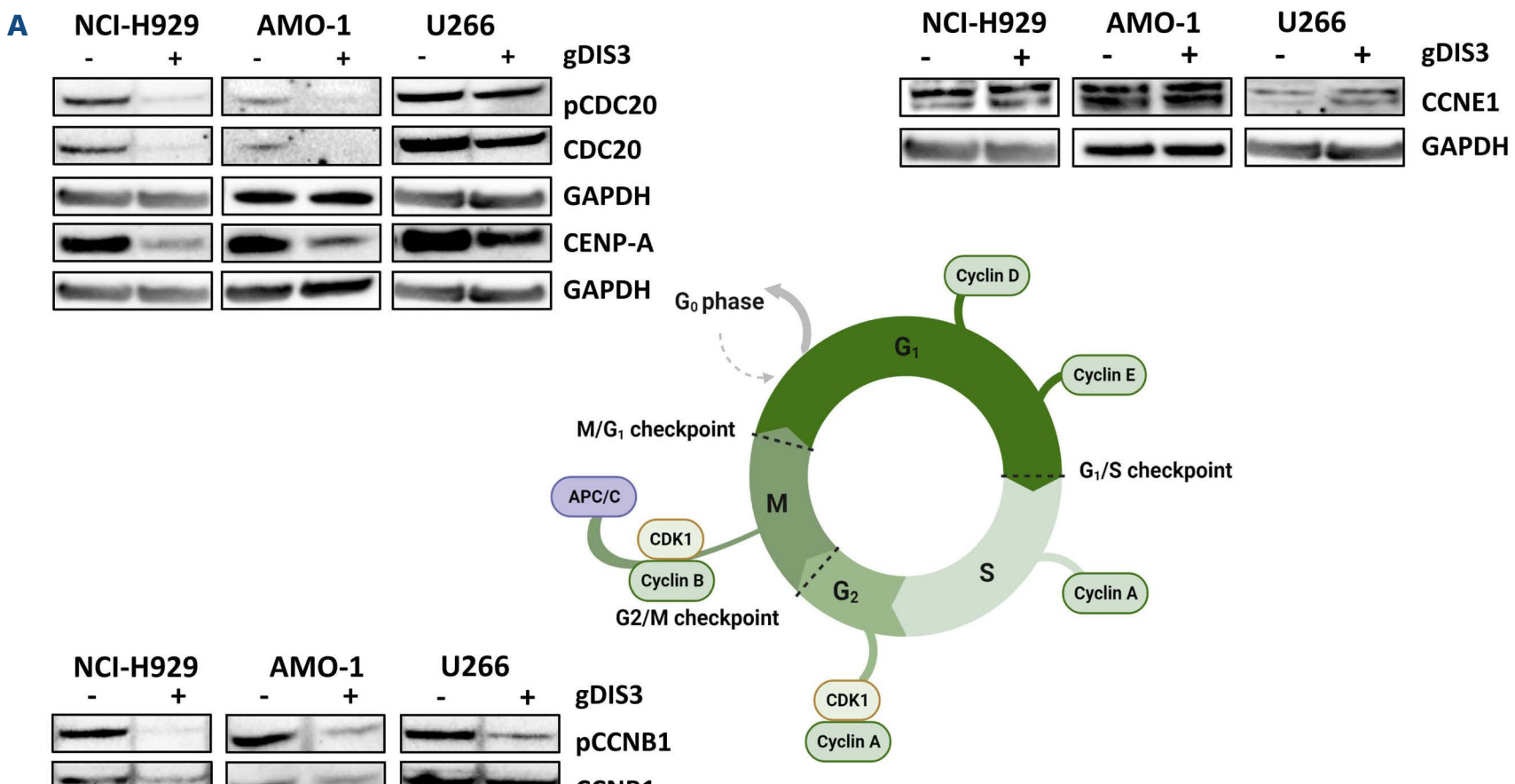

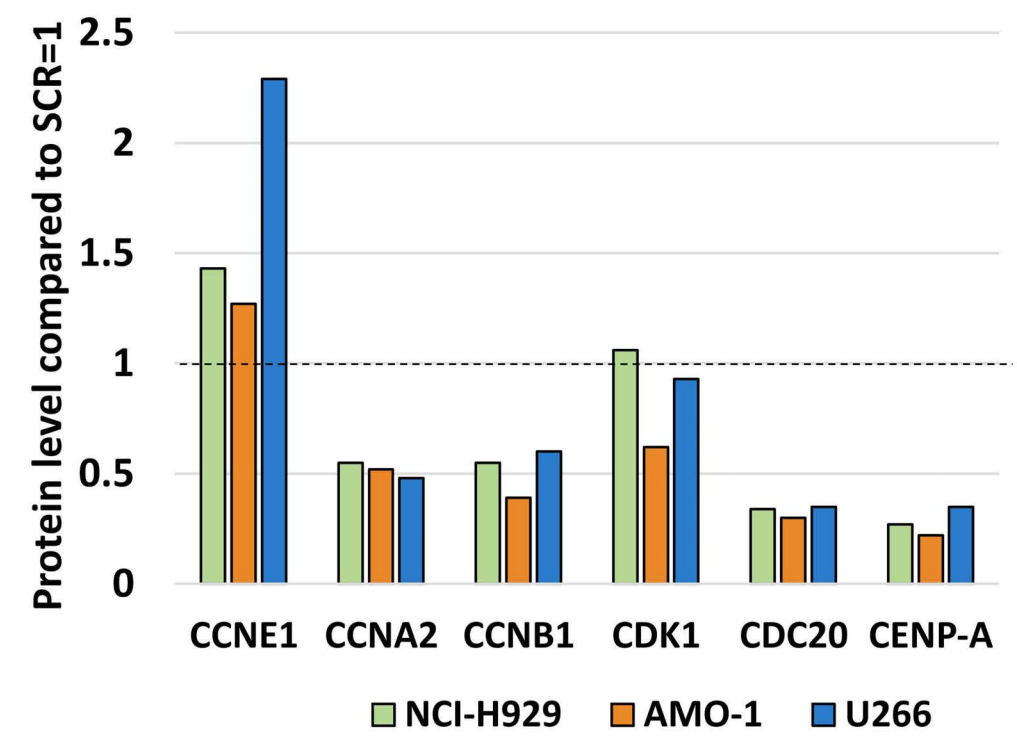

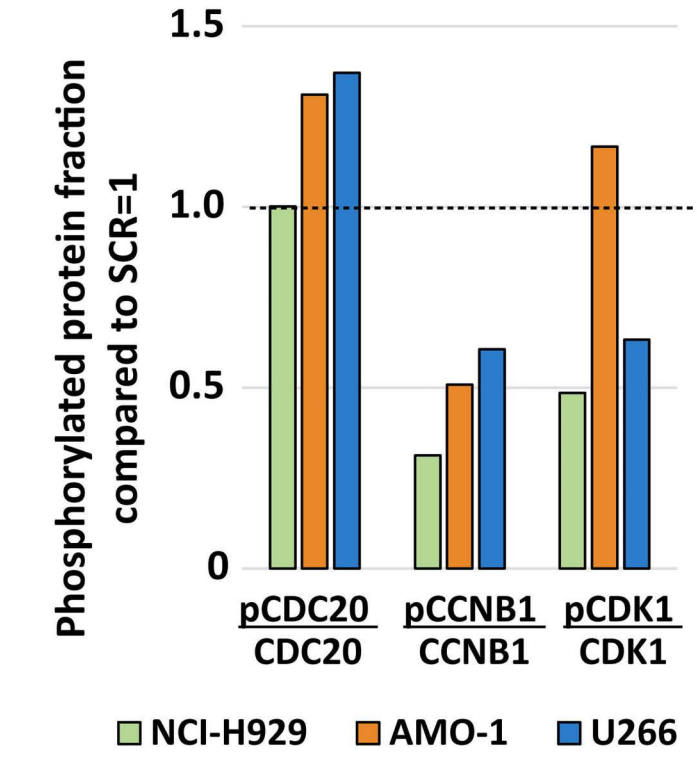

Figure 5. Western blot analyses of cell cycle checkpoint proteins. (A) Analysis performed in synchronized AMO-1, NCI-H929 and U266 cells 6 h after release. For NCI-H929 cells, pCDC20, CDC20 and CENP-A were evaluated on the same blot and thus with the same GAPDH control; to improve the overall symmetry of the figure and its comprehension, the same GAPDH panel has been reported twice. (B) Western blot results are quantified and plotted in a histogram. (C) Histogram of the modulation of the phosphorylated protein fraction upon g*DIS3* treatment, calculated as a ratio of phosphorylated protein to total protein in g*DIS3*-treated cells compared to the ratio of phosphorylated protein to total protein in scramble-treated ones. SCR: scramble condition.

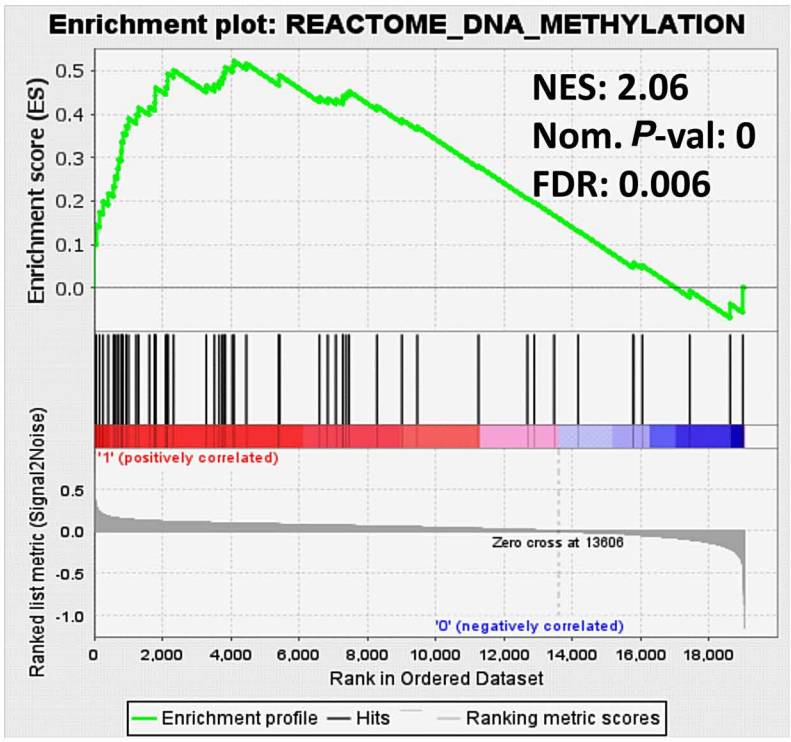

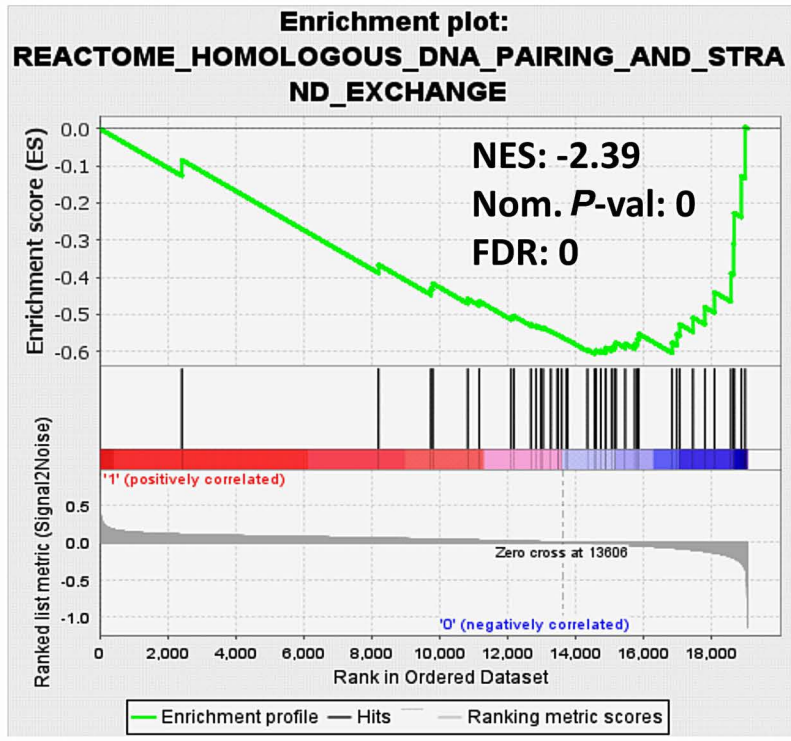

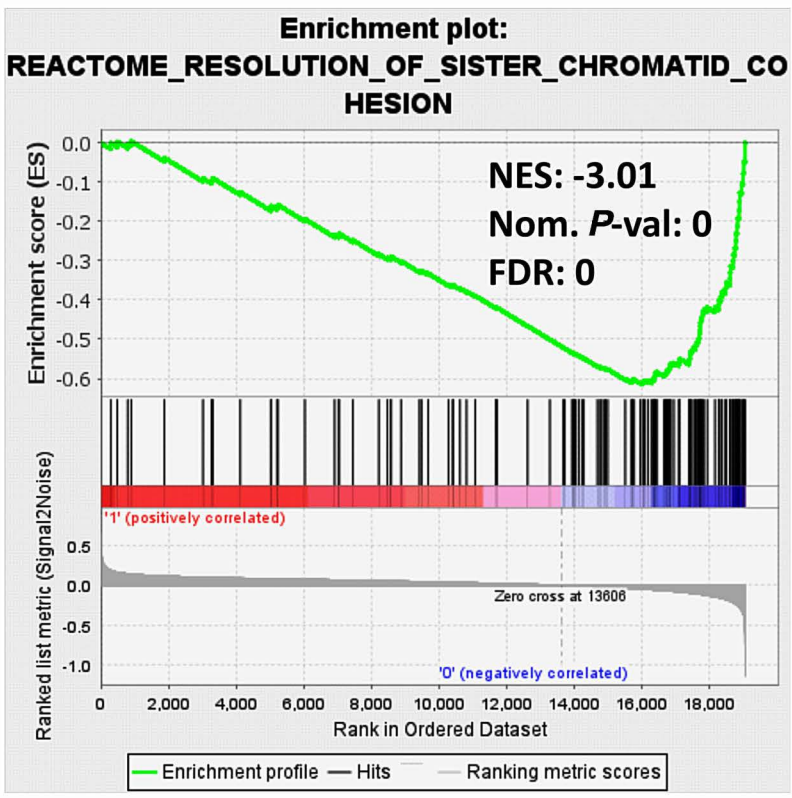

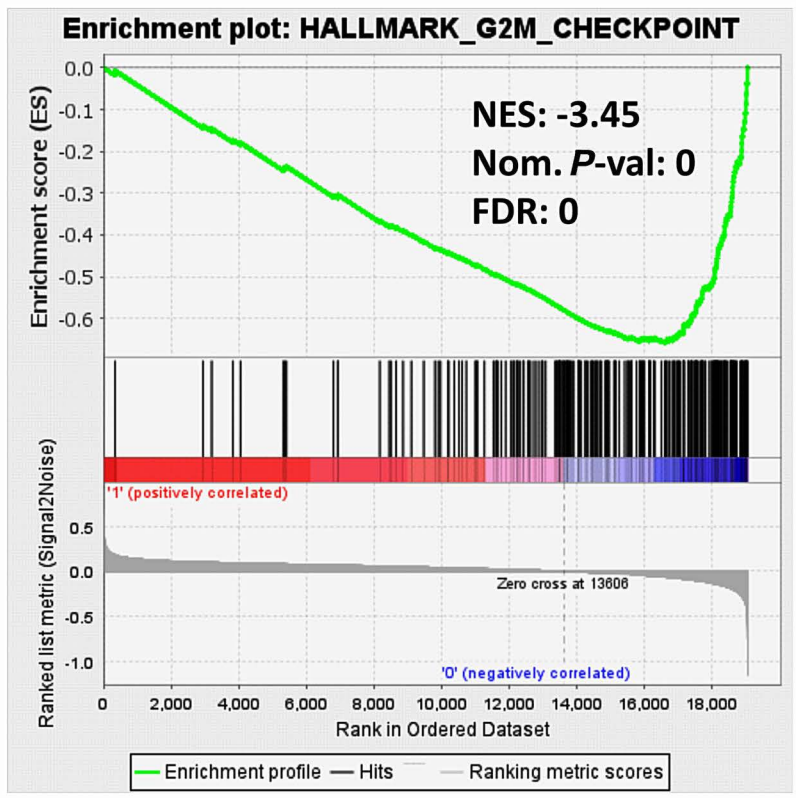

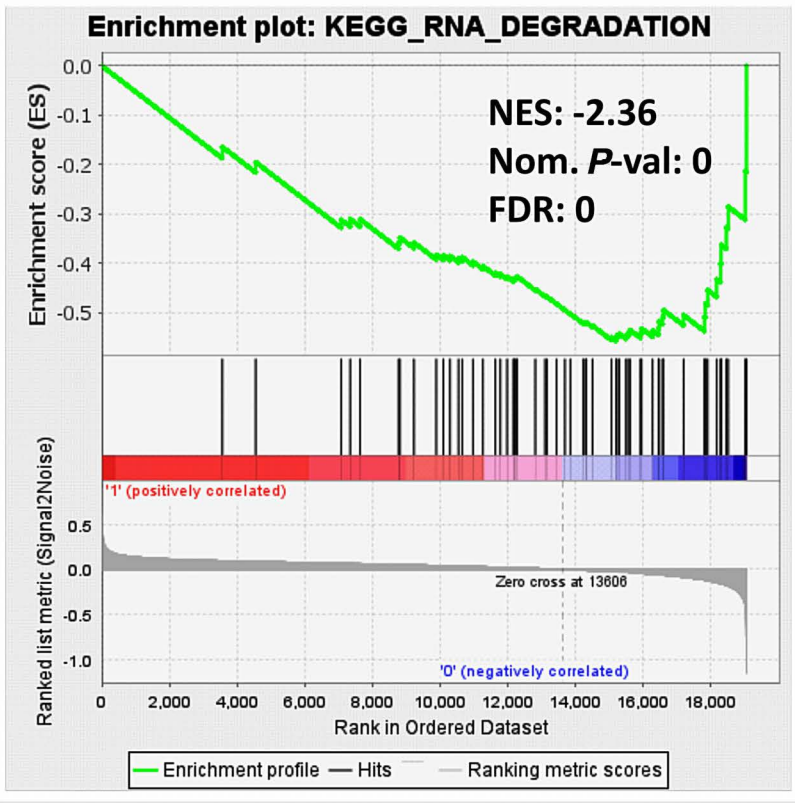

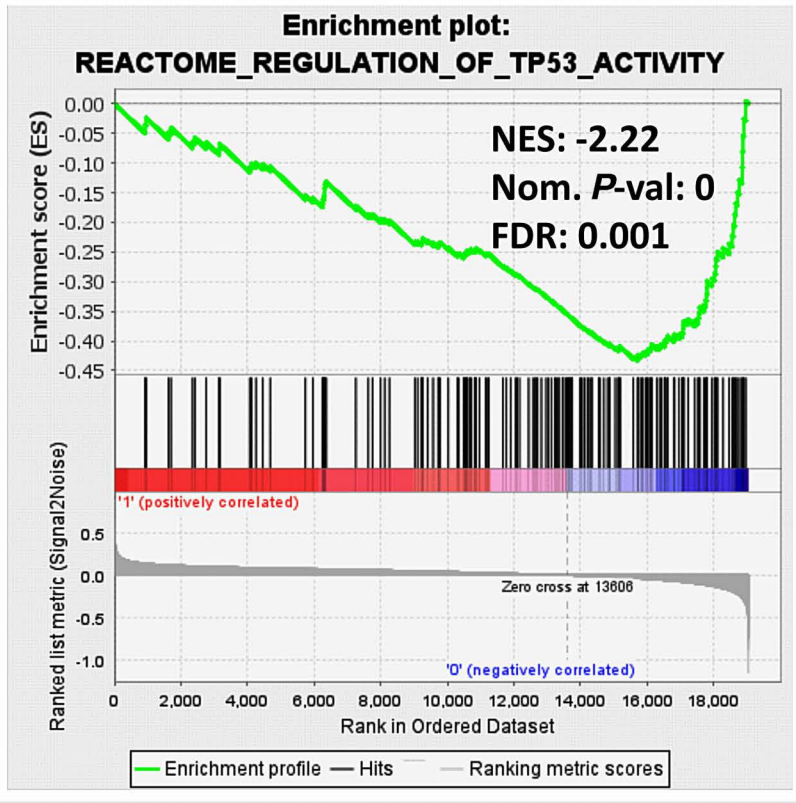

Continued on following page.

Figure 6. Transcriptomic analyses in *DIS3*-depleted cells. Enrichment plots of selected gene set enrichment analysis (GSEA) gene sets significantly modulated in *DIS3*-silenced cells in comparison to scrambled NCI-H929 cells. GSEA was performed on global annotated protein-coding gene expression profiles (19,048 genes) and the most significant gene sets were selected under stringent conditions (nominal *P* value <0.05 and false discovery rate *q* value <5%). The enrichment score and nominal *P* values are reported for each plot. NES: normalized enrichment score; FDR: false discovery rate.

Finally, to find possible molecular subsets of genes that were coordinately modulated in *DIS3*-silenced cells in comparison to control NCI-H929 cells, gene set enrichment analysis was performed on global annotated protein coding gene expression profiles and the most significant gene sets were selected under stringent conditions (nominal *P* value <0.05 and false discovery rate *q* value <5%) (*Online Supplementary Table S4*). Among the most significantly upregulated gene sets in *DIS3*-silenced NCI-H929 cells, some were involved in degradation of extracellular matrix and DNA and histone epigenetic modifications, whereas cell cycle checkpoint, chromosome organization, RNA processing and degradation, DNA recombination and repair, regulation of TP53 activity and numerous cell signaling pathways resulted among the most significantly underexpressed gene sets in *DIS3*-silenced cells (Figure 6, *Online Supplementary Table S4*).

Based on our evidence that *DIS3* can regulate cell cycle, chromosome organization and DNA repair processes, we validated the expression of some genes involved in these processes by means of quantitative real-time polymerase chain reaction in *DIS3*-silenced AMO-1, NCI-H929, and U266 cell lines. In particular, we considered *RAD51B* and *ARID5B*, which are involved in homologous recombination and DNA repair processes; in addition, we investigated *CCNB1*, *CDC20*, the microtubule motor protein *KIF14*, the DNA topoisomerase *TOP2A* and the RNA polymerase *POLR2H*, all of which are involved in the cell cycle process. All these genes resulted downregulated upon *DIS3* silencing in all cell lines (Figure 7A). The downregulation of these genes was also validated *ex-vivo* in *DIS3*-depleted primary CD138$^+$ tumor cells, except for *CCNB1* and *CDC20*, likely because purified PC hardly duplicate (Figure 7B).

DIS3 depletion affects mitotic spindle organization and the geometry of multiple myeloma cells

Considering previously reported data in yeast and *Drosophila* indicating that *DIS3*-KD can affect chromosome segregation and spindle assembly, and based on our evidence that *DIS3*-KD in HMCL leads to a decrease of CENP-A, which is fundamental for the proper formation of the mitotic spindle, we investigated whether *DIS3* depletion could affect mitotic spindle formation also in MM PC.

To obtain a significant number of mitotic cells to analyze, *DIS3*-KD cells were synchronized at the M phase of the cell cycle (Figure 8A). In detail, cells were immunostained for *DIS3*, centrosomes (γ-tubulin), and mitotic spindle fibers (α-tubulin), and nuclei were counterstained with DAPI. Notably, we found that *DIS3* silencing leads to the formation of supernumerary centrosomes accompanied by important changes in mitotic spindle organization and geometry in HMCL. Hence, in contrast to control cells which displayed normal spindle localization and physiological bipolar cell division, *DIS3*-KD cells showed the presence of multipolar spindles during mitosis (Figure 8B, C, *Online Supplementary Figure S13*).

Discussion

Aberrant expression of *DIS3* has been described in different tumors types, including MM. Of note, the frequent and almost specific occurrence of *DIS3* mutations observed in MM influences the clinical outcome of the patients.[3] However, the pattern of *DIS3* expression and its functional and pathogenic role in PC malignancies has not yet been clarified. In this study, we investigated the effects of *DIS3* depletion in myeloma cells, providing insights into its putative role in the pathobiology of the disease.

First of all, we explored *DIS3* expression in patients affected by MM or PCL and found that pathological samples expressed higher *DIS3* transcript levels than those of normal controls; indeed, even in patients carrying del13, despite their loss of heterozygosity, the amount of *DIS3* transcript did not fall below the levels of normal controls. Our analysis showed that *DIS3* expression levels did not influence the clinical outcome of MM in patients included in the CoMMpass dataset; however, this result could be affected by the fact that the group with low *DIS3* expression level was largely enriched in cases with del13 and/or t(4;14), whereas the group with higher *DIS3* expression level was enriched in patients with t(11;14) and/or hotspot *DIS3* mutations (*Online Supplementary Figure S2*). Overall, these data suggest that the co-occurrence of different molecular alterations in MM patients could mask the specific oncogenic function of *DIS3* expression in the disease.[32]

We, therefore, investigated the biological role of *DIS3 in vitro* by exploiting a loss-of-function approach in HMCL. Our experiments revealed that *DIS3*-KD largely affects cell cycle progression in MM cells, leading to a decrease in the fraction of cells distributed in the S and G2/M phases, and a consistent increase of cells in the G0/G1 phase. These findings strongly suggest that *DIS3* plays an important role in the control of the G1 phase of the cell cycle. In agreement with this idea, we found that in the CoMMpass da-

taset, MM patients with t(11;14) and high expression levels of CCND1, which is necessary for the transition from the G1 to the S phase of the cell cycle, were those significantly associated with the highest DIS3 expression levels (*Online Supplementary Figure S1*).

The prominent role of *DIS3* in the G1 phase is also suggested by the fact that in different cell types, including HMCL, *DIS3*-KD gives rise to a pervasive accumulation of DNA:RNA hybrids.[25] R-loops are three-stranded structures generated by the annealing of nascent transcripts to the template DNA strand and play important roles in physiological processes; however, uncontrolled hybrid production or lack of their immediate resolution through protein complexes, including RNases, helicases, and topoisomerases, can induce DNA damage and genome instability.[33] Importantly, the inhibition of the key homologous recombination factor RAD51 leads to accumulation of DNA:RNA hybrids in the early G1 phase of the cell cycle,[34] indicating that R-loop metabolism mainly occurs in the G1 phase.

Our results showed that *DIS3* plays an important role not only in the control of cell cycle in MM cells, but also in the centrosome duplication cycle, which are strictly coregulated in physiological conditions in the G1 phase of the cell cycle.[35,36] Indeed, for the first time we identified that *DIS3*-KD leads to the formation of supernumerary centrosomes which finally result in altered and multipolar mitotic spindles in the M phase of the cell cycle of MM cells. The requirement of *DIS3* RNase activity for proper mitotic cell division and correct chromosome condensation has been already described in yeast and *Drosophila melanogaster* models.[21,22,37-39] In addition, *S. pombe DIS3* mutants have been shown to have elongated metaphase spindles and a

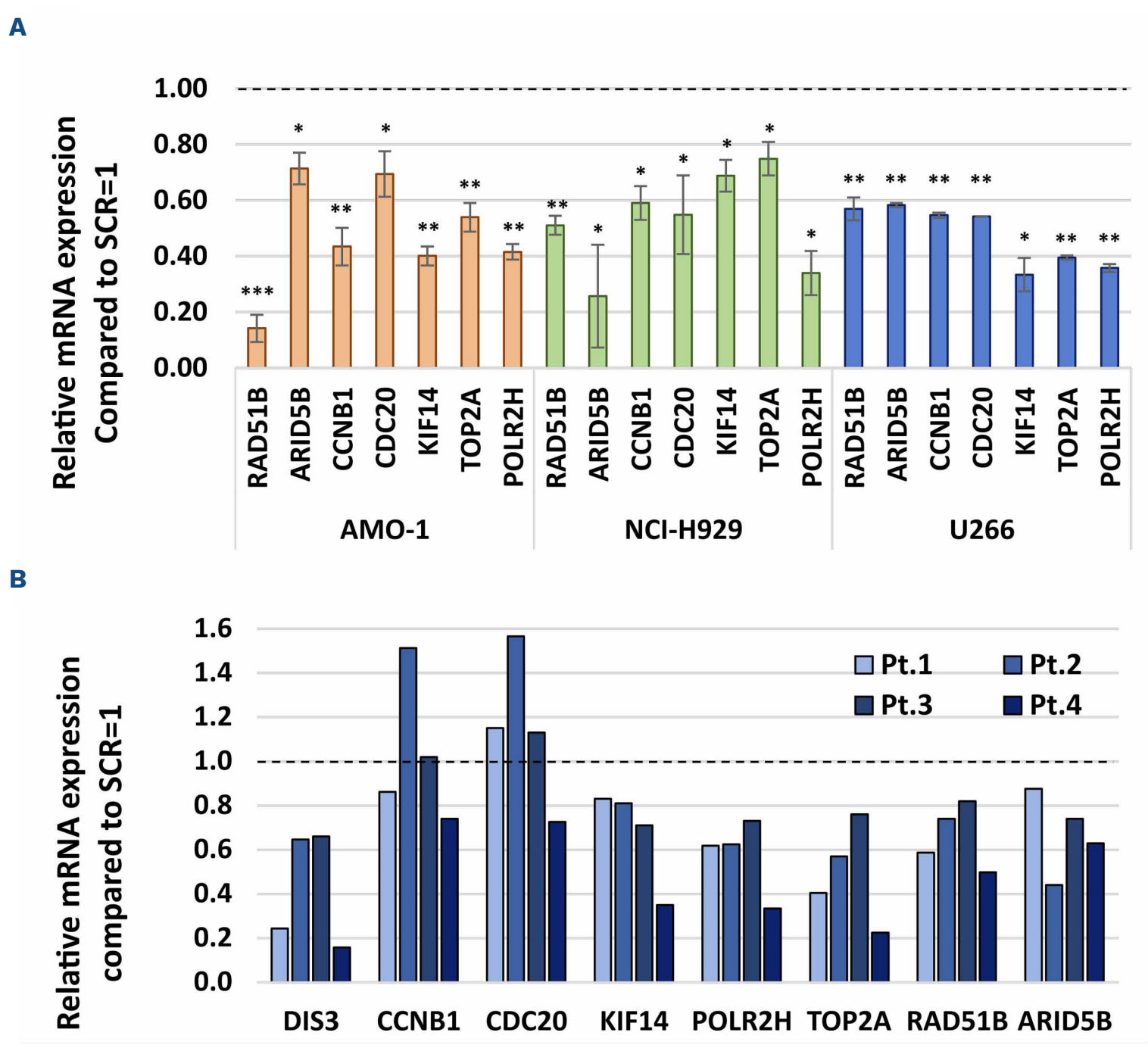

Figure 7. Molecular validation of the transcriptomic analysis. (A) Quantitative real-time polymerase chain reaction validation of the indicated genes in *DIS3*-depleted AMO-1, NCI-H929, and U266 human multiple myeloma cell lines; gene expression is presented as $2^{-\Delta\Delta Ct}$ relative to the *GAPDH* housekeeping gene and the scrambled condition used as a calibrator. **P*<0.05, ***P*<0.01, ****P*<0.001, Student *t* test. (B) *Ex-vivo* validation of the indicated genes in *DIS3*-depleted primary CD138$^+$ tumor cells purified from four multiple myeloma patients. SCR: scrambled condition.

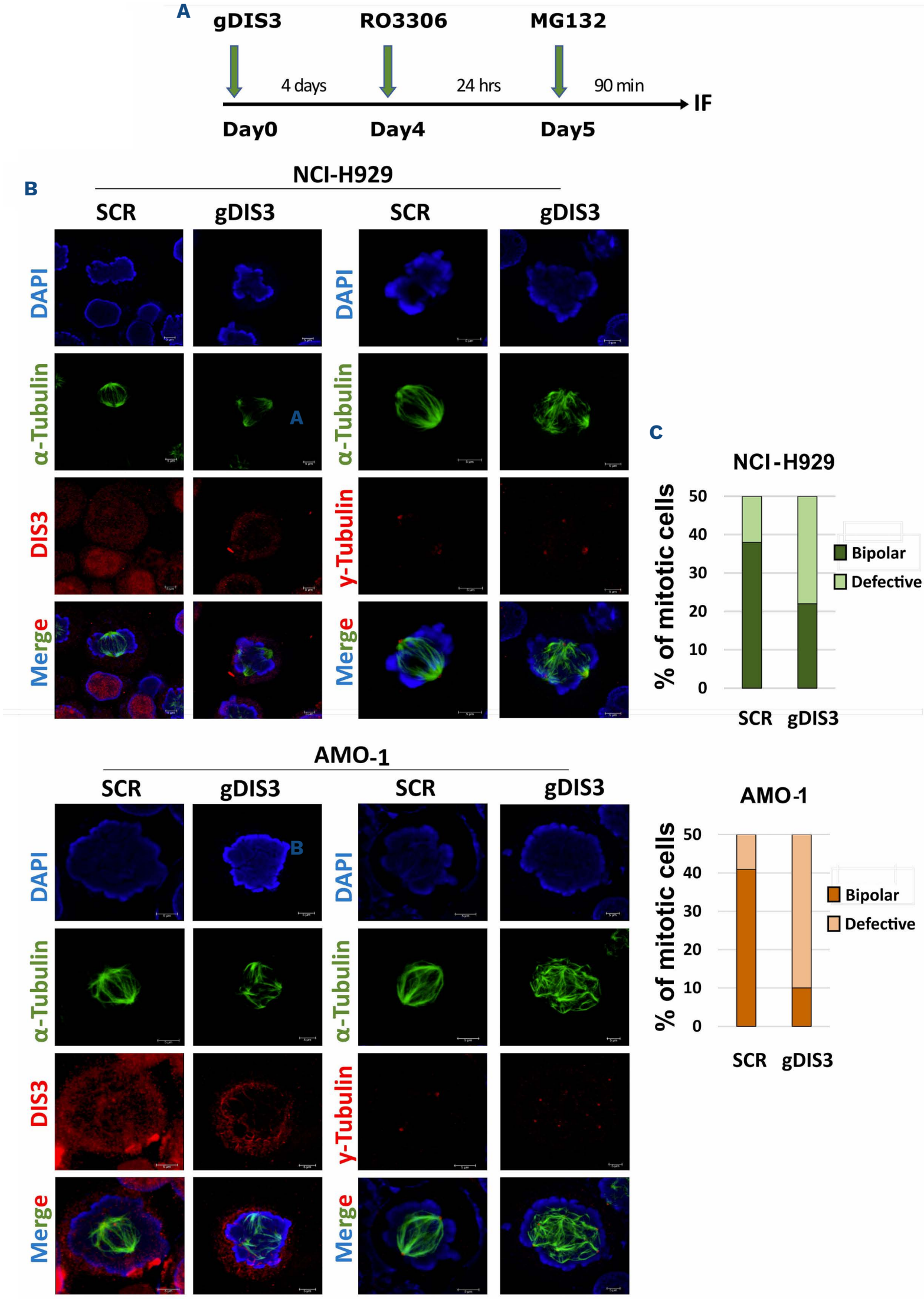

Figure 8. Images of metaphase spindles in NCI-H929 and AMO-1 cells treated with g*DIS3* or scrambled gapmer. (A) Schematic representation of the experimental setup used to synchronize cells. (B) Representative images of multipolar spindles in both cell lines following *DIS3*-knockdown (right panel for each cell line). Scale bar, 5 μm. (C) Percentage of mitotic cells with defective spindles in NCI-H929 and AMO-1 cells treated with g*DIS3 versus* scrambled gapmer. IF: immmunofluorescence; SCR: scrambled condition.

block in metaphase to anaphase transition.[22] Smith *et al.* provided further evidence that *DIS3* is involved in mitotic progression by demonstrating that perturbation of *DIS3* in *S. cerevisiae* affects microtubule localization and structure.[21] In MM PC, we found that *DIS3* could impact mitotic spindle formation by affecting centrosome duplication.

Numerical and/or structural centrosome amplification is a hallmark of solid tumors and hematologic malignancies and is often associated with aberrant tumor karyotypes and poor clinical outcomes.[40,41] In MM, centrosome amplification is present in about a third of patients and may represent a mechanism leading to genomic instability.[42] However, the clinical impact of centrosome amplification in MM is still debated and existing contradictory results may be explained by the clonal heterogeneity of MM in which each myeloma subclone with centrosome amplification may be potentially associated with different clinical behaviors influenced by complex processes including mitotic dysregulation, apoptotic failure and chromosome instability.[43,44]

The molecular mechanism by which *DIS3*-KD could induce formation of supernumerary centrosomes remains to be elucidated. These mechanisms might involve consecutive rounds of centrosome reproduction, or concurrent formation of daughter centrioles around the existing centrioles, or via *de novo* centrosome assembly independent of pre-existing centrioles.[40] Our transcriptional analysis revealed that genes involved in cell cycle checkpoint and chromosome organization were among the most significantly underexpressed ones in *DIS3*-silenced cells (Figure 6, *Online Supplementary Table S4*). Moreover, genes involved in serine/threonine protein kinase activity, with helicase function, catalytic activity on RNA, or with tubulin-binding function were evidenced in the top 20 remarkably enriched Gene Ontology Molecular Function terms upon *DIS3* silencing (*Online Supplementary Figure S11B*). In particular, several protein-coding genes that were significantly enriched in multiple annotation categories linked in complex interactions, regarding chromosome organization and nuclear division, or molecular activities on nucleic acids and tubulin, resulted globally downregulated in *DIS3*-silenced cells. Specifically, the downregulation of *KIF14*, *TOP2A* and *POLR2H*, all involved in cell cycle processes, has been validated *in vitro* and *ex vivo*.

Our transcriptomic analysis also showed that genes involved in DNA methylation were overexpressed in *DIS3*-silenced cells. This finding is in agreement with the observation that most of the mRNA expression level is reduced after *DIS3*-KD despite *DIS3* having ribonuclease activity, suggesting that global gene downregulation may be a secondary effect of *DIS3* deficiency on DNA methylation.

Overall, our data prompt further studies to clarify the role of *DIS3* in the process of centrosome duplication; indeed, a combination of *DIS3* defects and deficient spindle-assembly checkpoint, already described in MM,[45] can allow cells to progress through the cell cycle without proper chromosome segregation, thus generating aneuploid cells which may lead to the development of MM.

Disclosures

No conflicts of interest to disclose.

Contributions

VKF, ET, IS, GF, VT, NP, FT, KT, VF, and DR performed experiments and analyzed the data. VKF, ET, DG, and IS performed cytofluorimetric experiments. ET, VKF, and SE performed the confocal analysis, NB, NM, EM AC, RC, PF, and YT provided critical evaluation of experimental data and of the manuscript. DR, VKF, ET, and AN conceived the study and wrote the manuscript.

Funding

This work was financially supported by grants from the Associazione Italiana Ricerca sul Cancro (AIRC) to AN (IG24365), to ET (MFAG 2022-ID.27606) and to RC (IG20614). NB is funded by the European Research Council under the European Union's Horizon 2020 research and innovation program (grant agreement n. 817997) and by the Associazione Italiana Ricerca sul Cancro (IG25739). YT acknowledges support from "Piattaforme cellulari per la Ricerca e lo Sviluppo di Terapie Avanzate in Life Science" - Fondo Europeo di Sviluppo Regionale 2014-2020 (POR FESR 2014-2020). VKF received a fellowship through the PhD program in Experimental Medicine of the University of Milan. NP received a fellowship through the PhD program in Clinical and Experimental Medicine of the University of Modena and Reggio Emilia. The work was partially founded by the Italian Ministry of Health (Current Research IRCCS).

Data-sharing statement

Data are available from the corresponding author upon reasonable request.

References

1. Munshi NC, Anderson KC. New strategies in the treatment of multiple myeloma. Clin Cancer Res. 2013;19(13):3337-3344.
2. Morgan GJ, Walker BA, Davies FE. The genetic architecture of multiple myeloma. Nat Rev Cancer. 2012;12(5):335-348.
3. Todoerti K, Ronchetti D, Favasuli V, et al. DIS3 mutations in multiple myeloma impact the transcriptional signature and clinical outcome. Haematologica. 2022;107(4):921-932.
4. Lionetti M, Barbieri M, Todoerti K, et al. A compendium of DIS3 mutations and associated transcriptional signatures in plasma cell dyscrasias. Oncotarget. 2015;6(28):26129-26141.

5. Boyle EM, Ashby C, Tytarenko RG, et al. BRAF and DIS3 mutations associate with adverse outcome in a long-term follow-up of patients with multiple myeloma. Clin Cancer Res. 2020;26(10):2422-2432.
6. Bolli N, Avet-Loiseau H, Wedge DC, et al. Heterogeneity of genomic evolution and mutational profiles in multiple myeloma. Nat Commun. 2014;5:2997.
7. de Groen FLM, Krijgsman O, Tijssen M, et al. Gene-dosage dependent overexpression at the 13q amplicon identifies DIS3 as candidate oncogene in colorectal cancer progression. Genes Chromosomes Cancer. 2014;53(4):339-348.
8. Weißbach S, Langer C, Puppe B, et al. The molecular spectrum and clinical impact of DIS3 mutations in multiple myeloma. Br J Haematol. 2015;169(1):57-70.
9. Ng D, Toure O, Wei MH, et al. Identification of a novel chromosome region, 13q21.33-q22.2, for susceptibility genes in familial chronic lymphocytic leukemia. Blood. 2007;109(3):916-925.
10. Rose AE, Poliseno L, Wang J, et al. Integrative genomics identifies molecular alterations that challenge the linear model of melanoma progression. Cancer Res. 2011;71(7):2561-2571.
11. Binder M, Rajkumar SV, Ketterling RP, et al. Prognostic implications of abnormalities of chromosome 13 and the presence of multiple cytogenetic high-risk abnormalities in newly diagnosed multiple myeloma. Blood Cancer J. 2017;7(9):e600.
12. Chiecchio L, Dagrada GP, Ibrahim AH, et al. Timing of acquisition of deletion 13 in plasma cell dyscrasias is dependent on genetic context. Haematologica. 2009;94(12):1708-1713.
13. Tomecki R, Kristiansen MS, Lykke-Andersen S, et al. The human core exosome interacts with differentially localized processive RNases: hDIS3 and hDIS3L. EMBO J. 2010;29(14):2342-2357.
14. Schneider C, Leung E, Brown J, Tollervey D. The N-terminal PIN domain of the exosome subunit Rrp44 harbors endonuclease activity and tethers Rrp44 to the yeast core exosome. Nucleic Acids Res. 2009;37(4):1127-1140.
15. Tomecki R, Drazkowska K, Kucinski I, et al. Multiple myeloma-associated hDIS3 mutations cause perturbations in cellular RNA metabolism and suggest hDIS3 PIN domain as a potential drug target. Nucleic Acids Res. 2014;42(2):1270-1290.
16. Mitchell P, Petfalski E, Shevchenko A, Mann M, Tollervey D. The exosome: a conserved eukaryotic RNA processing complex containing multiple 3′→5′ exoribonucleases. Cell. 1997;91(4):457-466.
17. Wasmuth EV, Lima CD. Exo- and endoribonucleolytic activities of yeast cytoplasmic and nuclear RNA exosomes are dependent on the noncatalytic core and central channel. Mol Cell. 2012;48(1):133-144.
18. Kinoshita N, Goebl M, Yanagida M. The fission yeast dis3+ gene encodes a 110-kDa essential protein implicated in mitotic control. Mol Cell Biol. 1991;11(12):5839-5847.
19. Ohkura H, Adachi Y, Kinoshita N, Niwa O, Toda T, Yanagida M. Cold-sensitive and caffeine-supersensitive mutants of the Schizosaccharomyces pombe dis genes implicated in sister chromatid separation during mitosis. EMBO J. 1988;7(5):1465-1473.
20. Noguchi E, Hayashi N, Azuma Y, et al. Dis3, implicated in mitotic control, binds directly to Ran and enhances the GEF activity of RCC1. EMBO J. 1996;15(20):5595-5605.
21. Smith SB, Kiss DL, Turk E, Tartakoff AM, Andrulis ED. Pronounced and extensive microtubule defects in a Saccharomyces cerevisiae DIS3 mutant. Yeast Chichester Engl. 2011;28(11):755-769.
22. Murakami H, Goto DB, Toda T, et al. Ribonuclease activity of Dis3 is required for mitotic progression and provides a possible link between heterochromatin and kinetochore function. PloS One. 2007;2(3):e317.
23. Hou D, Ruiz M, Andrulis ED. The ribonuclease Dis3 is an essential regulator of the developmental transcriptome. BMC Genomics. 2012;13:359.
24. Szczepińska T, Kalisiak K, Tomecki R, et al. DIS3 shapes the RNA polymerase II transcriptome in humans by degrading a variety of unwanted transcripts. Genome Res. 2015;25(11):1622-1633.
25. Gritti I, Basso V, Rinchai D, et al. Loss of ribonuclease DIS3 hampers genome integrity in myeloma by disrupting DNA:RNA hybrid metabolism. EMBO J. 2022;41(22):e108040.
26. Taiana E, Favasuli V, Ronchetti D, et al. Long non-coding RNA NEAT1 targeting impairs the DNA repair machinery and triggers anti-tumor activity in multiple myeloma. Leukemia. 2020;34(1):234-244.
27. Matthews HK, Bertoli C, de Bruin RAM. Cell cycle control in cancer. Nat Rev Mol Cell Biol. 2022;23(1):74-88.
28. Musacchio A, Salmon ED. The spindle-assembly checkpoint in space and time. Nat Rev Mol Cell Biol. 2007;8(5):379-393.
29. Bruno S, Ghelli Luserna di Rorà A, Napolitano R, Soverini S, Martinelli G, Simonetti G. CDC20 in and out of mitosis: a prognostic factor and therapeutic target in hematological malignancies. J Exp Clin Cancer Res CR. 2022;41(1):159.
30. Lub S, Maes A, Maes K, et al. Inhibiting the anaphase promoting complex/cyclosome induces a metaphase arrest and cell death in multiple myeloma cells. Oncotarget. 2016;7(4):4062-4076.
31. Pesenti ME, Raisch T, Conti D, et al. Structure of the human inner kinetochore CCAN complex and its significance for human centromere organization. Mol Cell. 2022;82(11):2113-2131.
32. Bolli N, Biancon G, Moarii M, et al. Analysis of the genomic landscape of multiple myeloma highlights novel prognostic markers and disease subgroups. Leukemia. 2018;32(12):2604-2616.
33. Santos-Pereira JM, Aguilera A. R loops: new modulators of genome dynamics and function. Nat Rev Genet. 2015;16(10):583-597.
34. Nascakova Z, Boleslavska B, Urban V, et al. RAD51 inhibition induces R-loop formation in early G1 phase of the cell cycle. Int J Mol Sci. 2021;22(7):3740.
35. Prigent C, Uzbekov R. Duplication and segregation of centrosomes during cell division. Cells. 2022;11(15):2445.
36. Lin M, Xie SS, Chan KY. An updated view on the centrosome as a cell cycle regulator. Cell Div. 2022;17(1):1.
37. Graham AC, Kiss DL, Andrulis ED. Core exosome-independent roles for Rrp6 in cell cycle progression. Mol Biol Cell. 2009;20(8):2242-2253.
38. Robinson SR, Oliver AW, Chevassut TJ, Newbury SF. The 3' to 5' exoribonuclease DIS3: from structure and mechanisms to biological functions and role in human disease. Biomolecules. 2015;5(3):1515-1539.
39. Snee MJ, Wilson WC, Zhu Y, et al. Collaborative control of cell cycle progression by the RNA exonuclease Dis3 and Ras is conserved across species. Genetics. 2016;203(2):749-762.
40. Mittal K, Kaur J, Jaczko M, et al. Centrosome amplification: a quantifiable cancer cell trait with prognostic value in solid malignancies. Cancer Metastasis Rev. 2021;40(1):319-339.
41. Krämer A, Neben K, Ho AD. Centrosome aberrations in hematological malignancies. Cell Biol Int. 2005;29(5):375-383.
42. Chng WJ, Fonseca R. Centrosomes and myeloma; aneuploidy and proliferation. Environ Mol Mutagen. 2009;50(8):697-707.
43. Dementyeva E, Kryukov F, Kubiczkova L, et al. Clinical implication of centrosome amplification and expression of centrosomal functional genes in multiple myeloma. J Transl Med. 2013;11:77.
44. Kryukova E, Kryukov F, Hajek R. Centrosome amplification and clonal evolution in multiple myeloma: short review. Crit Rev Oncol Hematol. 2016;98:116-121.
45. Díaz-Rodríguez E, Álvarez-Fernández S, Chen X, et al. Deficient spindle assembly checkpoint in multiple myeloma. PloS One. 2011;6(11):e27583.